Science of the Total Environment 927 (2024) 172297

Contents lists available at ScienceDirect

Science of the Total Environment

journal homepage: www.elsevier.com/locate/scitotenv

Valorization of steelmaking slag and coal fly ash as amendments in combination with *Betula pubescens* for the remediation of a highly As- and Hg-polluted mining soil

S. Sánchez [a,b], D. Baragaño [c,*], J.R. Gallego [b], M.A. López-Antón [c], R. Forján [b,d], A. González [a]

[a] Department of Organisms and Systems Biology, Area of Plant Physiology IUBA, University of Oviedo, Catedrático Rodrigo Uría s/n, 33006 Oviedo, Asturias, Spain
[b] Environmental Biogeochemistry and Raw Materials Group, University of Oviedo, Campus de Mieres, Gonzalo Gutiérrez Quirós s/n, 33600 Mieres, Asturias, Spain
[c] Instituto de Ciencia y Tecnología del Carbono, INCAR-CSIC, Francisco Pintado Fe, 26, 33011 Oviedo, Spain
[d] Plant Production Area, Department of Biology of Organisms and Systems Biology, University of Oviedo, 33600 Mieres, Spain

HIGHLIGHTS

- By-products immobilize As and Hg in soil, reducing their accumulation in plants
- Fertilizers boost plant growth & raise As accumulation; by-products mitigate uptake
- Birch enhances thiolic compounds production in response to pollutants accumulation
- Hg in leachates is retained as chloride in fly-ash within the permeable barrier

GRAPHICAL ABSTRACT

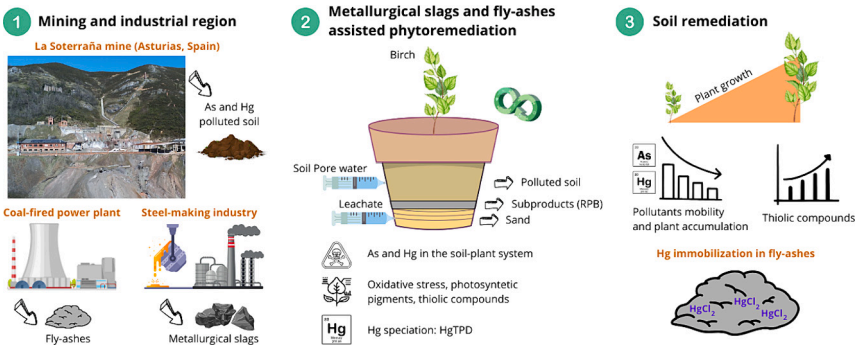

ARTICLE INFO

Keywords:
Soil pollution
Arsenic
Mercury
Circular economy
Phytoremediation

ABSTRACT

Soil pollution by As and Hg is a pressing environmental issue given their persistence. The intricate removal processes and subsequent accumulation of these elements in soil adversely impact plant growth and pose risks to other organisms in the food chain and to underground aquifers. Here we assessed the effectiveness of non-toxic industrial byproducts, namely coal fly ash and steelmaking slag, as soil amendments, both independently and in conjunction with an organic fertilizer. This approach was coupled with a phytoremediation technique involving *Betula pubescens* to tackle soil highly contaminated. Greenhouse experiments were conducted to evaluate amendments' impact on the growth, physiology, and biochemistry of the plant. Additionally, a permeable barrier made of byproducts was placed beneath the soil to treat leachates. The application of the byproducts reduced pollutant availability, the production of contaminated leachates, and pollutant accumulation in plants, thereby promoting plant development and survival. Conversely, the addition of the fertilizer alone led to an increase in As accumulation in plants and induced the production of antioxidant compounds such as carotenoids and free proline. Notably, all amendments led to increased thiolic compound production without affecting chlorophyll synthesis. While fertilizer application significantly decreased parameters associated with oxidative stress, such as hydrogen peroxide and malondialdehyde, no substantial reduction was observed after byproduct application.

* Corresponding author.
E-mail address: diego.baragano@incar.csic.es (D. Baragaño).

https://doi.org/10.1016/j.scitotenv.2024.172297
Received 30 January 2024; Received in revised form 23 March 2024; Accepted 5 April 2024
Available online 7 April 2024

Thermal desorption analysis of the byproducts revealed Hg immobilization mechanisms, thereby indicating retention of this metalloid in the form of Hg chloride. In summary, the revalorization of industrial byproducts in the context of the circular economy holds promise for effectively immobilizing metal(loid)s in heavily polluted soils. Additionally, this approach can be enhanced through synergies with phytoremediation.

1. Introduction

Mining and metallurgical activities cause significant metal(loid) pollution. In addition, inadequate waste management and the abandonment of these activities over the past few decades have led to the emergence of extensive contaminated brownfields containing metal (loid)s and other pollutants (Hudson-Edwards, 2016; Boente et al., 2022; Fernández et al., 2020). In the European Union, it is estimated that 2.8 million sites are potentially affected by metal(loid) pollution, and of these about 14 % require urgent soil restoration (Payá-Peréz and Rodríguez-Eugenio, 2018). In this regard, pollution by metal(loid)s, specifically arsenic (As) and mercury (Hg), is one of the most relevant environmental concerns worldwide. The uptake and accumulation of these metal(loid)s in plants pose a serious risk as they can enter the trophic chain and cause major health and environmental problems (FAO and ITPS, 2015; Chandrakar et al., 2016; Natasha et al., 2020; Janeiro-Tato et al., 2021; Zhang et al., 2021). Moreover, the contamination of surrounding soil and groundwater through leaching is an additional concern, particularly when these resources are used by nearby communities (Wang et al., 2022; Triassi et al., 2023). As stated in the Minamata Convention, there is a global need to reduce the contamination caused by As and Hg, especially the latter, and thus protect public health (Evers et al., 2016).

Phytoremediation involves plants that can absorb and accumulate pollutants in their tissues. In addition, plants that inhabit contaminated lands provide organic matter and nutrients, which in turn contribute to the recovery and stabilization of soil fertility (Jacob et al., 2018; Aparicio et al., 2022). These accumulator plants use two distinct strategies to handle metal(loid) toxicity, namely avoidance and tolerance (Viehweger, 2014). On the other hand, toxicity caused by metal(loid) entry into the cytosol is reduced through chelation by binding of heavy metal ions to ligands and subsequent compartmentalization of these complexes, mainly in vacuoles (Mohan et al., 2016; Yan et al., 2020). These chelating complexes include glutathione (GSH), phytochelatins (PCs), metallothioneins, amino acids such as histidine or proline, and certain low molecular weight organic acids, such as citric and malic acid (Viehweger, 2014; Souri et al., 2017; Bortoloti and Baron, 2022). In addition to chelating metal ions, GSH is a precursor of PCs, which are non-protein thiols (NPTs) synthesized by several molecules of GSH that bind free metal ions by producing a high content of thiolic groups (-SH) (Jozefczak et al., 2012; Zagorchev et al., 2013; Dennis et al., 2019).

Metal(loid) accumulation in the cytosol causes stress, which is characterized by the synthesis of free radicals and reactive oxygen species (ROS) (Sytar et al., 2013; Taran et al., 2020). Excessive ROS blocks functional groups of biomolecules, disrupts metabolic pathways, and also damages proteins, the integrity of lipid membranes, and above all DNA (Berni et al., 2019). To reduce the oxidative damage caused by metal(loid)s and to cope with their toxicity, plants have developed a complex network of detoxification mechanisms (Viehweger, 2014), which involve antioxidant enzymes, such as catalase and peroxidase (Bhaduri and Fulekar, 2012; Fernández et al., 2013; Leão et al., 2014; Gąsecka et al., 2021), and antioxidant compounds, such as phenolic compounds like carotenoids, amino acids like proline, and GSH (Jozefczak et al., 2012; Mourato et al., 2012; Mishra et al., 2016).

In the context of soil pollution by metal(loid)s, in recent decades, there has been a focus on combining nature-based techniques with distinct amendments. The latter chemically interact with pollutants and increase the efficiency of soil remediation, thereby enhancing the immobilization or mobilization of soil pollutants (Baragaño et al., 2022; Gąsecka et al., 2021; Gil-Díaz et al., 2019; Lebrun et al., 2021). Furthermore, the possibility of using industrial byproducts as soil amendment fully conforms with the principles of the circular economy (Breure et al., 2018), thereby creating added value for material such as steelmaking waste, coal slag, and fly ash (Bashir et al., 2019; Ayala and Fernández, 2020; Liu et al., 2020). However, the impact of these different materials on plants is still unknown. It is therefore pertinent to study the effects of these byproducts on plants before their inclusion in phytoremediation efforts.

Here we assessed the efficacy of local and non-toxic industrial byproducts, specifically coal fly ash and steelmaking slag, as amendments to immobilize As and Hg in a contaminated mining soil. The study included a phytoremediation approach, focusing on the impact of these materials on the growth, physiology, and biochemistry of *Betula pubescens* (birch). To this end, we aimed to: 1) evaluate the metal(loid) bioavailability and leachability; 2) analyse the growth, metal(loid) accumulation, thiolic compounds, and physiological and oxidative-stress parameters in plants and 3) decipher the mechanisms behind Hg immobilization.

2. Materials and methods

2.1. Site history

Asturias (northern Spain) is a region with a long history of mining and metallurgical activities, which were of considerable relevance until the 1970s. Consequently, the present landscape is characterized by numerous brownfields greatly impacted by pollutants, including metal (loid)s and organic contaminants (Gallego et al., 2015; González-Fernández et al., 2018). In particular, “La Soterraña”, located in the Muñón-Cimero valley (Asturias), is a former Hg mine which was of significant importance until its closure in 1974 (Ayala and Fernández, 2020; Fernández et al., 2020). The development of these activities and the dumping of several types of mining-metallurgical waste material has impacted the environmental compartments and the surroundings have been widely affected by As and Hg pollution (Baragaño et al., 2022; Boente et al., 2022; Fernández et al., 2020; Matanzas et al., 2017).

2.2. Soil sampling and amendments

To conduct the remediation feasibility study, a 20 kg sample from the first 30 cm of soil in “La Soterraña” was collected. Once in the laboratory, the soil was air-dried, mixed in a concrete mixer to maximize homogeneity, and then passed through a 2-mm sieve.

Several amendments were used in this study. Sourced from Italpollina (Verona, Italy), Phenix is an organic fertilizer comprising animal manure and plant debris and it has a N:P:K ratio of 6:8:15. Additionally, the industrial byproducts, namely coal fly ash and steelmaking slag, were provided by EDP Energy and Escorias y Derivados S.A. (EDERSA), respectively. The motivation for using these materials stems from their large-scale generation within the region. As they are non-toxic, they have traditionally been stockpiled or disposed of, however, there is now a growing need to find sustainable solutions for their management. Both materials were characterized in a previous study (Fernández et al., 2020) and basic characterization is shown in Table S1. However, the coal fly ash was subjected to an exhaustive characterization due to their great capacity to retain Hg from flue gases (Abad-Valle et al., 2011). The organic matter content was determined as loss on ignition (LOI), which was identified as the weight loss experienced by the sample when

incinerated at 815 °C following ISO 1171 standard procedures. Furthermore, surface area was determined using the BET (Brunauer-Emmett-Teller) method after performing physical adsorption isotherms of N_2 at 77 K on a Micromeritics ASAP 2420 volumetric adsorption system, following sample degassing for 12 h at 250 °C.

2.3. Plant material

Betula pubescens (birch) was chosen based on previous findings (Fernández-Fuego et al., 2017b; Lebrun et al., 2021) that demonstrated its notable tolerance of and resistance to highly contaminated soils. Additionally, this species has a robust root system and substantial biomass. A selected *B. pubescens* clone was maintained in vitro in Murashige and Skoog medium (pH 5.7) (Murashige and Skoog, 1962) in a growth chamber at 25 °C and a 16 h light/8 h dark photoperiod for 2 months, until the radical system had developed. The plants were then acclimated through a fog tunnel for 20–30 days to gradually reduce their humidity and adapt their physiology to natural environmental conditions, and they were finally transferred to uncontaminated soil. The shoot and root length, and fresh weight of each plant were measured before plants were transferred to the 1 L pots used in two experiments performed under greenhouse conditions.

2.4. Experimental design

The first experiment was designed to evaluate not only the influence of the amendments on the soil-plant system but also to monitor the lixiviation of As and Hg from the soil and the feasibility of a reactive permeable barrier (RPB) to mitigate the presence of these two pollutants in the leachates. To this end, pots were filled with a 2 cm-layer of silica sand, followed by the untreated or treated polluted soil from "La Soterraña". Five pots were prepared for each treatment, with one plant planted per pot. The following three treatments were tested: only polluted soil, S1; soil amended with 12 g of organic fertilizer, S1F; and soil amended with 12 g of organic fertilizer and a mixture of byproducts (1:2, fly ash:slag) applied at a dose of 20%wt, S1FR. The mixture proportion was determined according to several tests (data not shown) to evaluate the permeability of the material since a high dose of coal fly ash was revealed as an inadequate amendment because of soil compaction. The mixture of materials with this proportion was maintained as soil amendments, akin to the approach used in the RPB study. This consistency ensured homogeneity and facilitated a comprehensive comparison of all the results obtained. Finally, a RPB was introduced into treatments S1F and S1FR, denoted as S1F + RPB and S1FR + RPB, respectively. The RPB comprised a 2-cm layer of a byproduct mixture designed to act as a permeable material, interacting with soil leachates to immobilize As and Hg. Beyond reducing the concentrations of these pollutants in leachates, this material served the dual purpose of remediating soil and elucidating the immobilization mechanisms of the amendments. To evaluate the capacity of the amendments to decrease As and Hg mobility, pore water (PW) samples were obtained from the soil. Furthermore, PW samples were also taken from the sand to evaluate the originated leachates. To this end, soil moisture samplers (Rhizon samplers) were placed at two levels: one in the soil layer and the other in the silica sand layer. The experiment lasted 7 days. A scheme of the experimental design is shown in Fig. 1.

The second experiment involved a mixture of the highly polluted soil (S1) and moderately polluted soil from the site in equal proportions to provide a less contaminated sample, designated as S2. This experiment involved 6 pots per treatment, with one plant planted per pot. The following treatments were tested: untreated soil (S2); soil with 6 g of fertilizer (S2F); soil with 20%wt of the byproduct mixture (S2R); and soil with 6 g of fertilizer and 20%wt of the byproduct mixture (S2RF). The experiment lasted 60 days. The scheme of the experimental design is shown in Fig. 1.

In both sets of experiments, to achieve soil stabilization, the polluted

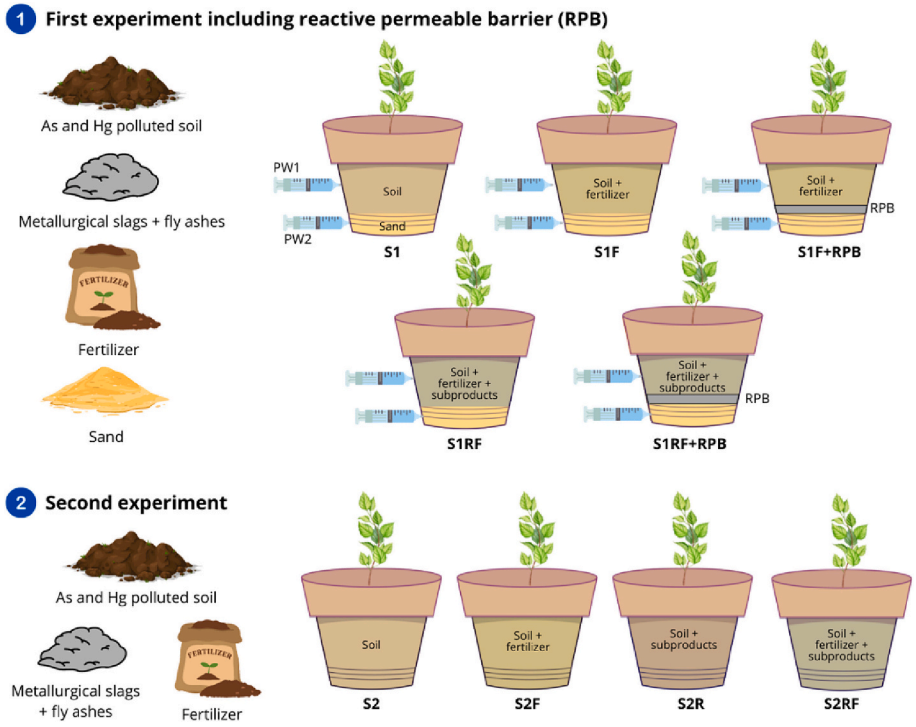

Fig. 1. Experimental design of the two pot experiments. 1) Illustrative scheme of pot experiments for the different treatments applied in soil S1: S1, highly contaminated soil; S1F, fertilizer-treated soil; S1F + BPR, fertilizer-treated soil with reactive permeable barrier (RPB); S1RF, fertilizer- and byproduct-amended soil; and S1RF + BPR, fertilizer- and byproduct-amended soil with RPB. Sand was placed at the bottom of the pots to collect leachates from the soil. Pore water samples (PW1 and PW2) were also collected. 2) Illustrative scheme of pot experiments for the different treatments applied in soil S2: S2, moderately contaminated soil; S2F, fertilizer-treated soil; S2R, byproduct-amended soil; S2RF, fertilizer- and byproduct-amended soil.

soils were treated with the amendments 3 days before transferring plants to the pots.

2.5. Soil and pore water samples

At the beginning and end of the experiment, the concentration of pseudo-total metal(loid)s was determined after acid digestion with a mixture of nitric and hydrochloric acids in a 1:3 ratio (v:v) in a microwave reaction system (Milestone ETHOS 1, Italy). The concentration of As, Cd, Cu, Fe, Pb, Zn, and Hg in the digestate was quantified by Inductively Coupled Plasma Mass Spectrometry (ICP-MS 7700; Agilent Technologies, California, USA). Available As and Hg were determined using the simple extraction "Toxicity Characteristic Leaching Procedure" (TCLP) (USEPA, 1992).

Pore water (PW) samples were collected at the end of the experiment using soil moisture samplers, and pH and electrical conductivity (EC) were then measured using a Mettler Toledo multimeter. Next, the As and Hg concentration in the samples was analysed by ICP-MS.

2.6. Plant growth and metal(loid) accumulation

After 7 days, plants grown in S1 were collected and washed with tap water and rinsed 3 times in deionized water for 5 min. Once the excess water had been dried with cellulose paper, the fresh weight, and shoot and root length were measured again to calculate the biomass rate using the following equation:

$$\text{Biomass rate} = (\text{Final weight} - \text{Initial weight})/\text{Initial weight} \quad (1)$$

Plants were then divided into leaves, stems, and roots, powdered using a cryogenic grinder (6775 Freezer/Mill® SPEX SamplePrep), and stored at −80 °C until further analysis. Since the amount of sample of each treatment obtained in this assay was very small, samples were used solely to measure metal(loid) content. Plants grown in S2 were collected after 60 days, and washed, divided, and stored in the same way as the previous experiment, until further analysis.

To determine the concentration of metal(loid)s in the plants, an aliquot of the shoots and roots was oven-dried at a temperature below 40 °C. Next, 200 mg of samples from each treatment was digested using 3 mL of concentrated HNO_3, and highly purified in a microwave oven for 6 min at 240 W. The digestion extracts were cooled and successive dilutions were made with deionized water and a solution of 10 μg kg^{-1} of Rh concentrated HNO_3 was added as an internal standard (Baragaño et al., 2022). The concentration of As and Hg in plant tissues was determined by ICP-MS.

The translocation factor (FT), enrichment factor (EF), and bioconcentration factor (BCF) were calculated following the equations described by Nirola et al. (2015):

$$\text{TF} = [\text{Metal(loid)}]_{\text{shoots}}/[\text{Metal(loid)}]_{\text{roots}} \quad (2)$$

$$\text{EF} = [\text{Metal(loid)}]_{\text{shoots}}/[\text{Metal(loid)}]_{\text{soil}} \quad (3)$$

$$\text{BCF} = [\text{Metal(loid)}]_{\text{roots}}/[\text{Metal(loid)}]_{\text{soil}} \quad (4)$$

2.7. Non-protein thiolic compounds in plants

The extraction and analysis of non-protein thiolic compounds (NPTs) were carried out from 300 mg of fresh leaves, and the stems and roots of *B. pubescens,* following the method described in Fernández et al. (2012). High-performance liquid chromatography (HPLC) separation was performed using a chromatograph Waters 600 (Waters Corporation) with a post-column derivatization with Ellman's reagent (Ellman, 1959). The sample (100 μL) was injected into a Kromasil 100 C18 5 μm (250× 4.6 mm) column (Scharlau) and eluted with solvent A (acetonitrile:H_2O, 2:98 (*v*/v) and 0.05 % trifluoroacetic acid (TFA)) and solvent B (acetonitrile:H_2O, 98:2 (v/v) also with 0.05 % TFA). Samples were separated using a linear gradient (0–25 % in 25 min and 25–50 % in 5 min) of solvent B at 1.5 mL min^{-1} flow for 30 min. The derivatized thiols were detected at 412 nm using Waters 996 photodiode array detector, and the peaks obtained were identified by comparison with the standards of GSH and a mix of PCs. The quantitative changes were analysed using the integration areas at 412 nm of absorbance converted into μmol g PF^{-1} and were quantified in terms of GSH equivalents.

2.8. Parameters related to oxidative stress

Chlorophyll and carotenoids were extracted from 500 mg of frozen leaves using 10 mL of 80 % acetone. Homogenates were centrifuged at 3000*g* for 10 min before measuring absorbance at 663, 646, and 470 nm. The pigment content was calculated following the equations of Lichtenthaler and Wellburn (1983) and expressed as μg g^{-1} fresh weight (FW):

$$Chlorophyll\ a\ (Ca) = 12.21\ Abs663 - 2.81\ Abs646 \quad (5)$$

$$Chlorophyll\ b\ (Cb) = 20.13\ Abs646 - 50.3\ Abs663 \quad (6)$$

$$Carotenoids = \frac{1000\ Abs470 - 3,27\ Ca - 104\ Cb}{229} \quad (7)$$

Chlorophyll fluorescence was measured with an OS1-FL portable fluorometer (Opti-Sciences) on the second fully expanded leaf, previously dark-adapted for 15 min. The Fv/Fm ratio was determined following the method described by Demmig-Adams and Adams (1996).

Hydrogen peroxide (H_2O_2) was measured following the method described by Singh et al. (2006), with some modifications. First, 100 mg of frozen leaves, stems or roots was homogenized with 2 mL of 0.1 % trichloroacetic acid (TCA) and centrifuged at 12000*g* for 15 min. Next, 0.5 mL of supernatant was mixed with 0.5 mL of 100 mM phosphate buffer (pH 7.6) and 1 mL of 1 M KI. The absorbance of the samples was measured at 390 nm and H_2O_2 content was determined using a standard curve and expressed as μmol g^{-1} FW.

Lipid peroxidation was determined by measuring the formation of malondialdehyde (MDA). First, 100 mg of frozen leaves, stems and roots was mixed with 2 mL of 0.1 % TCA following the method described by Demiral and Turkan (2005), with some modifications. The mixture was then centrifuged at 12000*g* for 15 min, and a 0.5 mL aliquot of the supernatant was added to 2 mL of 20 % TCA with 0.5 % thiobarbituric acid. The samples were heated at 95 °C for 25 min and cooled in an ice bath. Finally, the absorbance of the samples was measured at 532 and 600 nm ($\varepsilon = 155\ mM^{-1}\ cm^{-1}$). MDA content was determined using the Lambert-Beer equation and expressed as μmol g^{-1} FW.

$$MDA = \frac{Abs532 - Abs600}{\varepsilon} \quad (8)$$

Proline content was measured using the method described by Khedr et al. (2003), with some modifications. First, 100 mg of frozen leaves, stems and roots was homogenized with 1.5 mL of 3 % sulfosalicylic acid and centrifuged at 10000*g* for 10 min. Next, 0.5 mL of supernatant was mixed with 2 mL of acid ninhydrin and 2 mL glacial acetic acid (1:1, *v*/v) and heated in a water bath at 100 °C for 1 h. Samples were cooled in ice and 2.5 mL of toluene was added to the mixture. After the generation of two phases, the absorbance of the upper phase was measured at 520 nm. Proline content was determined using a standard curve and expressed as μmol g^{-1} FW.

2.9. Thermal desorption

The Hg species present in the RPB were identified using an Hg temperature-programmed desorption (HgTPD) device. Previously described by Rumayor et al. (2015), this device consists of a temperature-programmed furnace coupled to a PYRO 915 furnace from LUMEX and a continuous Hg analyser (RA-915). Desorption profiles are

obtained by heating the sample at a rate of 50 °C min^{-1}. The different desorption peaks obtained are assigned to each Hg species using the reference database of Hg compounds. We used HgS, $HgCl_2$, Hg_2Cl_2, and Hg-OM (mercury bound to organic matter) as references because they are the species most likely to be present or retained in coal fly ash (Abad-Valle et al., 2011).

2.10. Statistical analysis

All analytical determinations were performed in triplicate. The data obtained were statistically treated using SPSS programme, version 25.0 for Windows. Analysis of variance (ANOVA) and test of homogeneity of variance were carried out. In the case of homogeneity, a post hoc least significant difference (LSD) test was done. When there was no homogeneity, Dunnett's T3 test was performed.

3. Results and discussion

3.1. Physicochemical characterization of soil

The highly contaminated soil (S1) showed a slightly alkaline pH (Table S2), whereas the less polluted soil (S2) had a slightly acidic pH (Table S3). The addition of organic fertilizer led to a significant decrease in pH, contradicting the outcomes observed with other organic fertilizers, which showed either an increase in soil pH or no significant changes (Lin et al., 2019; Wang et al., 2020; Baragaño et al., 2022). In contrast, the pH increased after the application of the byproducts (Tables S1, S2)—an effect attributed to the alkaline pH of these amendments (fly ash pH 10.7; slag pH 11.9), which is shown in Table S1.

With regards to EC, all the amendments resulted in an increase in both S1 and S2 (Table S2), thereby suggesting that the addition of amendments is associated with a rise in EC. This finding is consistent with previous reports indicating that organic amendments, such as compost or biochar, increase EC through the release ions into the soil after watering (Lebrun et al., 2021). In neither treatment did EC exceed the values stipulated for soil to be considered saline and detrimental to plants (2 $dS{\cdot}m^{-1}$) (Hazelton and Murphy, 2007).

The untreated soils (S1 and S2) markedly exceeded the concentrations of As and Hg (Table S2) established by the Soil Screening Levels (SSL) for metal(loid)s in Asturias, 200 and 100 mg kg^{-1}, respectively, for industrial soil (BOPA, 2014). However, in both experiments, the application of byproducts led to a decrease in the total concentration of these two pollutants (Table S2) due to the dilution effect of adding a 20%wt dose.

3.2. Metal(loid) availability

Analysis of metal(loid) availability by TCLP showed that only around 6 % of total As was mobile (Table S3). However, Hg availability could not be determined by this method because the concentration of this metal was under the detection limit of the equipment (0.1 μg L^{-1}). As elucidated in a previous study (Janeiro-Tato et al., 2021), the low mobility of Hg in this soil is attributed to the presence of stable Hg species like cinnabar and metacinnabar. Consequently, measurements using TCLP may not accurately reflect Hg mobility; in contrast, PW monitoring proved to be a more suitable method for this purpose.

Metal(loid) availability is a crucial parameter in phytoremediation as it reflects the fraction of the total concentration that can be directly absorbed by roots, and, in the short-term, this availability is influenced by chemical and biological processes (Yan et al., 2020). In both experiments, the addition of amendments decreased the availability of As (Table S3). In the case of the byproducts, the reduction was higher (70 % in S1 and 50 % in S2) than that achieved after fertilizer application (Table S3). The addition of byproducts to water contaminated with metal(loid)s has been reported to cause a decrease in As (Ayala and Fernández, 2020). The immobilization of this metalloid is achieved mainly through its binding to calcium complexes present in the byproducts (whose concentration is around 40 % in slag) and subsequent precipitation (Wang and Tsang, 2013; Ayala and Fernández, 2020). With respect to Hg, the immobilization mechanism has not been addressed in the literature and is thus discussed in the last part of this section. Conversely, the addition of the fertilizer slightly reduced the availability of As in S1 (Table S3). This finding contradicts the results reported by Baragaño et al. (2022), where the application of phosphate or dissolved organic carbon through this fertilizer increased As availability, probably attributed to the alkaline pH of the soil S1 used in this work in opposite to the acidic soil used in the previous work.

PW samples from soil S1 (PW1) and sand (PW2) were analysed to evaluate As and Hg mobility and to simulate the generation of leachates that could reach unground aquifers vulnerable to superficial pollution. As expected, the results showed that the concentrations of As and Hg were higher in PW1 than in PW2, although there were significant differences between the soil treatments (Fig. 2A, B).

The application of fertilizer markedly increased the concentration of As and Hg in PW1 (Fig. 2A), thereby revealing a contrasting effect to what was observed using TCLP and aligning with the previous data. This discrepancy indicates that TCLP was not suitably applied for this treatment. Of note, As mobilization induced by the fertilizer was mitigated when byproducts were applied. Particularly noteworthy, the Hg concentration in PW1 showed a significant reduction following the application of byproducts, even when these were used in combination with the fertilizer.

On the other hand, the decrease in Hg and, to a lesser extent, As (Fig. 2B) observed in the leachate (PW2) resulted from the chemical

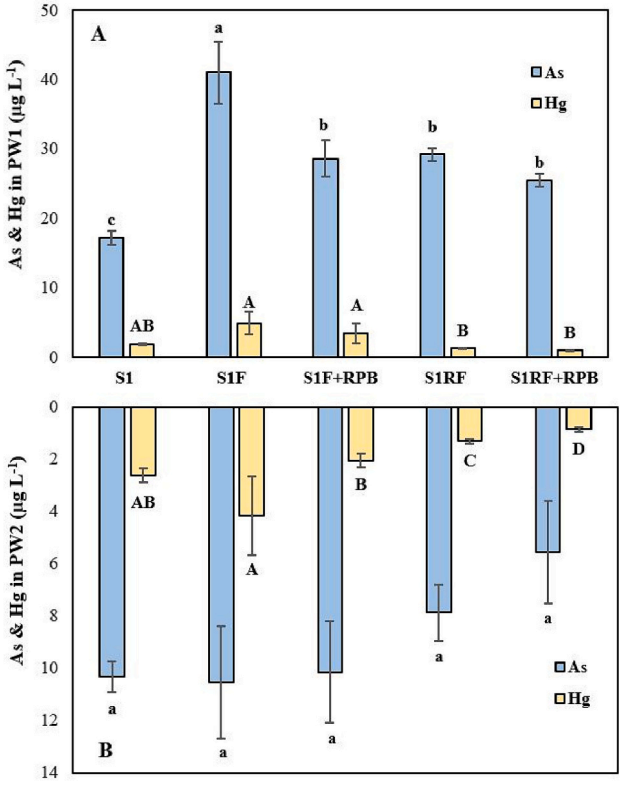

Fig. 2. Concentration of As and Hg (μg L-1) in pore water (PW) samples from A) soil, PW1, and B) sand, PW2, in the different soil treatments of highly contaminated soil S1. Different lower-case letters indicate significant differences between treatments for As and capital letters indicate significant differences between treatments for Hg. S1, highly contaminated soil; S1F, fertilizer-treated soil; S1F + BPR, fertilizer-treated soil with reactive permeable barrier (RPB); S1RF, fertilizer- and byproduct-amended soil; and S1RF + BPR, fertilizer- and byproduct-amended soil with RPB.

interaction of byproducts from the RPB (Ayala and Fernández, 2020). Consequently, the analysis of PW enabled observation of the effectiveness of the RPB to mitigate the generation of contaminated leachates.

These results highlight the capacity of steelmaking slag and coal fly ash to immobilize metal(loid)s (Medina et al., 2010; Wang and Tsang, 2013; Ayala and Fernández, 2020) and reveal their potential application in RPBs for the removal of As and Hg from polluted water. However, further research is essential to fully implement this barrier for water treatment.

3.3. Plant growth

Analysis of the growth parameters and biomass revealed the great capacity of *B. pubescens* to adapt and tolerate the presence of high concentrations of metal(loid)s in the soil. However, the appearance of plants grown in S1 deteriorated from day 3, showing symptoms of decay such as lack of hydration and necrosis. After 7 days, the experiment had to be terminated as plants in the S1F and S1F + RPB treatments had already perished. Furthermore, the other treatments continued to show distinct signs of turgor loss, deterioration, and necrosis (Fig. S1A).

In contrast, most of the plants grown in S2 were resilient to the various treatments over 60 days, except for S2F and S2RF, where only 50 % and 0 % of the plants survived, respectively (Fig. S1B). Although the metal(loid) concentration in this soil was much lower than S1, the toxicity was sufficiently high in some treatments to prevent survival or increase mortality, as was the case of the treatments that included fertilizer.

A reduction in fresh biomass was observed in all the soil treatments (Fig. 3A). This finding is attributed mainly to a reduction in the plant water content—a parameter that affects the photosynthetic machinery and metabolic activity of plants (Rucinska-Sobkowiak, 2016; Abbas et al., 2018; Baragaño et al., 2022). Similarly, the RPB did not facilitate effective water drainage, resulting in some waterlogging of the roots.

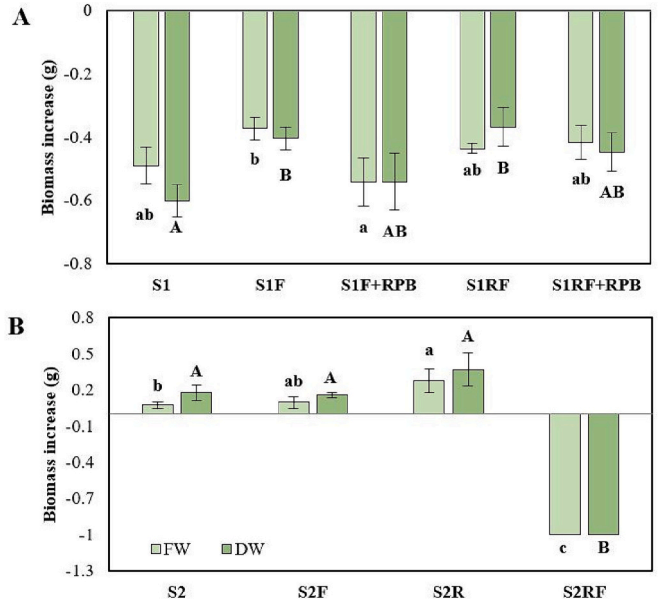

Fig. 3. Fresh biomass (FW) and dry biomass (DW) of *B. pubescens* after 7 days in highly contaminated soil S1 (A) and after 60 days in less contaminated soil S2 (B). Different lower-case letters indicate significant differences between treatments for FW and different capital letters indicate significant differences between treatments for DW. S1, highly contaminated soil; S1F, fertilizer-treated soil; S1F + BPR, fertilizer-treated soil with reactive permeable barrier (RPB); S1RF, fertilizer- and byproduct-amended soil; S1RF + BPR, fertilizer- and byproduct-amended soil with RPB. S2, moderately contaminated soil; S2F, fertilizer-treated soil; S2R, byproduct-amended soil; S2RF, fertilizer- and byproduct-amended soil.

This condition could potentially induce the synthesis of ethylene in leaves, leading to epinasty and, consequently, posing a threat to plant survival (León-Burgos et al., 2022). In contrast, the treatment that included byproducts (S2R) showed an increase in biomass production when compared with untreated soil (Fig. 3B) as a result of metal(loid) immobilization (Ayala and Fernández, 2020; Díaz et al., 2023).

3.4. As and Hg accumulation in plants

The accumulation of As surpassed that of Hg in both shoots and roots across all treatments, and the concentration in roots was consistently higher than in shoots (Fig. 4). This higher concentration was also observed by other authors in studies addressing a variety of plant species (Chen et al., 2015; González et al., 2019; Navazas et al., 2022). These results can be attributed to the fact that the root is the first organ in contact with the soil and the absorbed metal(loid)s are highly toxic and have no known function. Consequently, the plant promptly immobilizes them in cell walls or swiftly chelates and stores them in the cell vacuoles of the root to prevent harmful effects (Fernández et al., 2013; Souri et al., 2017; González et al., 2019; Lebrun et al., 2021).

In plants grown in S1, the highest As concentration in both shoots and roots was observed after fertilizer application (treatment S1F; Fig. 4A, B). This increase was due to the presence of high amounts of As in the PW (Fig. 2), thus facilitating absorption by the plant as As acts as an analogue of P and is absorbed by the same P transporter system (Lebrun et al., 2019; Navazas et al., 2021). The added fertilizer contains phosphate, which is more strongly adsorbed to the soil than As, and therefore competes for adsorption sites, thereby facilitating the release of As into the soil solution and thus its uptake by plants (Bolan et al., 2014; Lebrun et al., 2021; Baragaño et al., 2022). Likewise, the mobilization of As might also be due to the fact that organic fertilizers of animal origin, as in this case, contain substantial amounts of dissolved organic carbon, which could also mobilize some metalloids such as As (Souza Neto et al., 2020; Arabi et al., 2021). In all the treatments, the As concentration in roots exceeded 500 mg kg^{-1} after 7 days, while in shoots it exceeded 150 mg kg^{-1}, reaching 700 mg kg^{-1} in the S1F treatment (Fig. 4). These concentrations are extremely high and, according to White and Brown (2010), As concentrations ranging from 1 to 20 mg kg^{-1} can kill non-tolerant plants. Consequently, it is not surprising that the plants perished under these very high concentrations as this metalloid impairs numerous metabolic processes associated with photosynthesis, respiration, and nutrition (Mourato et al., 2019; Bali and Sidhu, 2021). Regarding Hg, a decrease in its accumulation was observed in the roots of plants grown in treated soils when compared with untreated soil (Fig. 4A), although no differences were observed across the treatments. (Fig. 4B). The Hg concentrations also exceeded the toxicity thresholds set between 2 and 5 mg kg^{-1} (White and Brown, 2010). Therefore, this Hg load, together with the high As concentrations, would explain the high plant mortality rate.

The significantly lower accumulation of As and Hg in the shoots of plants grown in S2 than in S1 (Fig. 4C) is in line with the observed higher survival rate of the former. Although the concentration of As and Hg was considerably lower in S2 than S1, it was four times higher than that considered toxic for a non-tolerant plant. This observation underscores the remarkable tolerance of *B. pubescens* to polluted soil (Fernández-Fuego et al., 2017a; Koptsik et al., 2021), as it survived despite the high accumulation of As in the roots, exceeding 400 mg kg^{-1} in all treatments (Fig. 4D). A comparison of the treatments reveals that the highest As concentration was in S2F plants, and like the previous assay, it would support metalloid mobilization by the fertilizer, making it more available for plant uptake and accumulation (Bolan et al., 2014; Lebrun et al., 2021). Regarding Hg accumulation, the highest concentration was observed in the shoots and roots of S2R plants (Fig. 4C, D). However, significant differences between treatments were not observed. Again, the concentration of the two metal(loid)s exceeded the toxicity thresholds set for non-tolerant plants (in the case of Hg, above 5 mg kg^{-1})

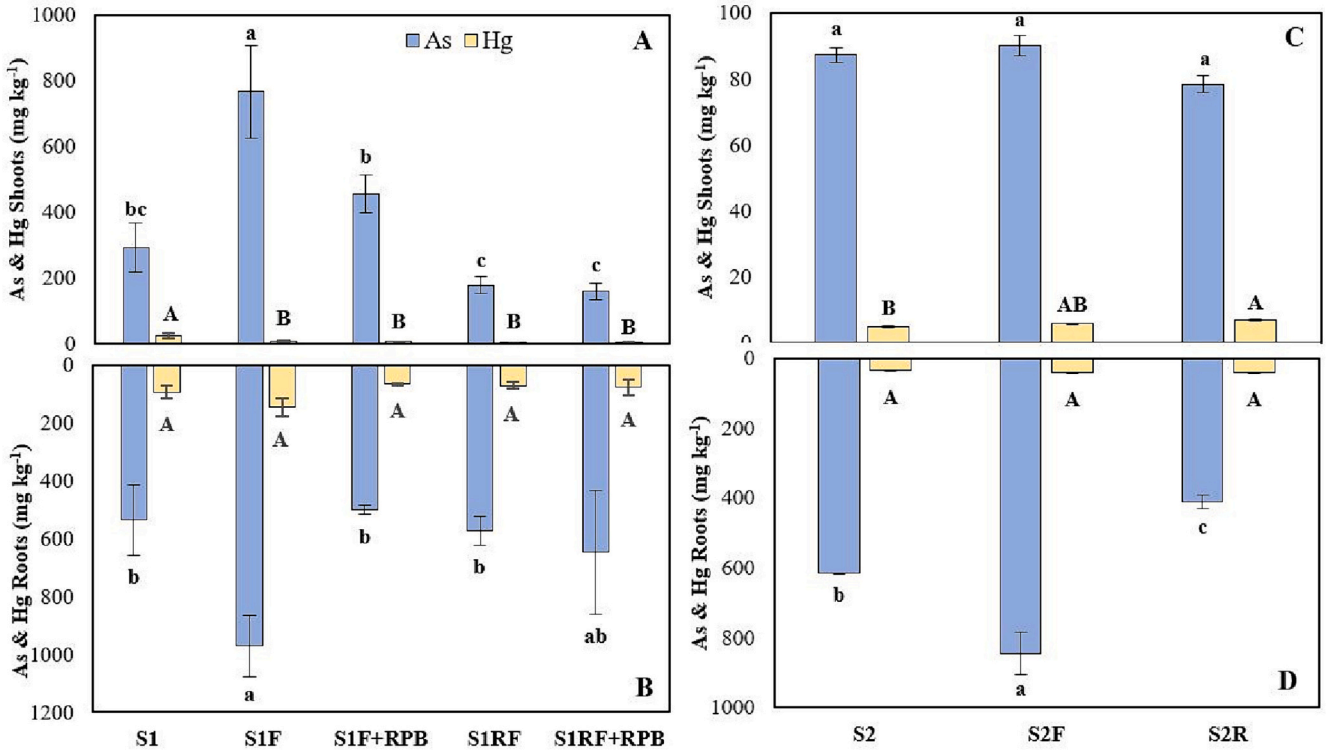

Fig. 4. As and Hg accumulation in shoots (A) and roots (B) of *B. pubescens* after 7 days growing in highly contaminated soil S1, and As and Hg accumulation in shoots (C) and roots (D) of *B. pubescens* after 60 days growing in less polluted soil S2. Different lower-case letters indicate significant differences between treatments for As and capital letters indicate significant differences between treatments for Hg. S1, highly contaminated soil; S1F, fertilizer-treated soil; S1F + BPR, fertilizer-treated soil with reactive permeable barrier (RPB); S1RF, fertilizer- and byproduct-amended soil; S1RF + BPR, fertilizer- and byproduct-amended soil with RPB. S2, moderately contaminated soil; S2F, fertilizer-treated soil; S2R, byproduct-amended soil; S2RF, fertilizer- and byproduct-amended soil.

(White and Brown, 2010). The great tolerance and resistance of birch is reflected by the high accumulation of As and Hg in its tissues.

For all treatments in S1, the translocation factor (TF), bio-concentration factor (BCF), and enrichment factor (EF) for As and Hg did not exceed 1 (Table S4). However, in the S1F and S1F + RPB treatments, there was a relevant As translocation rate towards the leaves (higher than 0.7). This finding indicates that a considerable part of the As absorbed by the roots was transported via the xylem to the leaves and redistributed to other parts of the plant (Bali and Sidhu, 2021; Zhang et al., 2021). In the case of S2, these parameters showed a similar trend to S1 (Table S4), thereby highlighting that S2R plants showed BCF and EF values for As higher than those of plants grown in the untreated soil (S2). The BCF and EF values for Hg in the two experiments (Table S4) could not be calculated because the available concentration of this metalloid could not be determined by TLCP, despite the detection of Hg in the shoots and roots (Fig. 4).

On the basis of our results, birch cannot be considered an As hyperaccumulator (Pasricha et al., 2021). However, it must be taken into account that contamination of the soil was extremely high and so the plants were unable to survive in some cases. On the other hand, some authors hypothesize that reduced metal(loid) translocation to aerial parts allows plants to avoid disruption of the photosynthetic system or other processes that could cause irreversible effects (Fernández et al., 2013; Souri et al., 2017; Mourato et al., 2019) and that it is also a strategy to prevent the entry of high concentrations of As and Hg into the trophic chain of edible plants (Sarwar et al., 2017). These results highlight the role of *B. pubescens* as an accumulator species which, with the addition of suitable amendments, could be used in phytostabilization assays for soils with extremely high concentrations of As and Hg.

3.5. Non-protein thiolic compounds

One of the mechanisms through which plants reduce the toxicity caused by cell absorption of metal(loid)s is via the synthesis of chelating compounds, such as PCs or other thiol compounds (CTs). The synthesis of such compounds is increased in response to greater exposure to metal (loid)s, thereby allowing the plant to reduce the toxic load caused by these contaminants and survive in these adverse conditions.

The analysis of phytochelatins and other thiol compounds was conducted solely on plants grown in less polluted soil (S2) as those in high polluted soil (S1) had perished by day 7. The results showed that in all the treatments, except in less polluted soil with fertilizer, the total concentration of non-protein thiols was higher in leaves than in shoots or roots (Table 1). In roots, the highest total thiol content was obtained in the polluted soil with fertilizer, doubling that in polluted soil and polluted soil with byproduct (Table 1). This increase was due mainly to de novo synthesis of cys-PC2, which was not present in the less polluted soil, and an increase in the production of desgly-PC3. This increase in the concentration of thiols in polluted soil with fertilizer was concomitant with the higher accumulation of As in the roots and also with the presence of Hg, although no differences in the accumulation of Hg were observed (Fig. 4D). A higher concentration of non-protein thiols upon the application of fertilizers was previously reported by various authors working with a range of plant species (Chen et al., 2015; González et al., 2019; Baragaño et al., 2022). The lowest thiol content was detected in the polluted soil with subproduct, which again matched the lowest As accumulation. Furthermore, this treatment was the only one in which PC4 was detected in roots. Conversely, PC6 appeared only in the roots of the polluted soil. Some studies (Pal and Rai, 2010; Sharma et al., 2016) argued that long-chain PCs contribute to more efficient detoxification as they have a greater ability to bind metal(loid)s and form more stable complexes, avoiding interaction with protein sulfhydryl groups, which

Table 1
Non-protein thiolic compounds (NPTs) (μmol g^{-1} FW) in the roots, shoots, and leaves of *B. pubescens* after 60 days growing in the different treatments of less polluted soil (S2). Different letters in the same row indicate significant differences between treatments. S2, moderately contaminated soil; S2F, fertilizer-treated soil; S2R, byproduct-amended soil.

NPTs	Roots			Shoots			Leaves		
	S2	S2F	S2R	S2	S2F	S2R	S2	S2F	S2R
GSH	1.65 ± 0.18a	0.17 ± 0.002c	0.98 ± 0.16b	2.04 ± 0.18a	0.3 ± 0.14b	0.87 ± 0.21b	6.65 ± 0.14a	0.91 ± 0.27b	4.6 ± 1.7a
CT1	–	–	–	–	–	–	–	0.35 ± 0.001a	–
desgly-PC2	0.22 ± 0.05b	0.5 ± 0.04a	–	–	–	0.35 ± 0.17a	–	–	–
cys-PC2	–	3.05 ± 0.05a	1.4 ± 0.09b	0.19 ± 0.1b	0.97 ± 0.08a	0.2 ± 0.03b	–	0.4 ± 0.02a	–
PC3	–	–	–	0.31 ± 0.03b	0.53 ± 0.01a	–	–	–	–
desgly-PC3	2.35 ± 0.05b	4.52 ± 0.05a	0.27 ± 0.17c	–	0.69 ± 0.18a	0.54 ± 0.34a	–	0.55 ± 0.03a	–
cys-PC3	–	–	–	–	–	–	3.55 ± 2.76a	2.05 ± 0.42a	4 ± 1.66a
PC4	–	–	0.56 ± 0.09a	0.15 ± 0.01a	0.2 ± 0.07a	–	–	–	–
PC6	0.19 ± 0.04a	–	–	–	–	–	–	–	–
CT2	–	–	–	–	–	–	–	0.73 ± 0.23a	–
CT3	–	–	–	–	–	–	–	0.22 ± 0.03a	–
Total CTs	4.41 ± 0.15b	8.24 ± 0.06a	3.21 ± 0.34c	2.69 ± 0.06a	2.7 ± 0.16a	1.96 ± 0.35a	10.63 ± 3.08a	5.19 ± 0.37a	8.6 ± 3.38a

could affect metabolism.

The lowest non-protein thiols concentration was observed in shoots, and no differences between treatments were detected (Table 1). These findings are consistent, as shoots, which serve as the intermediary transfer zone between roots and leaves, typically accumulate minimal amounts of metal(loid)s. The presence of thiols in shoots may indicate their participation in transportation to either leaves or roots.

Regarding leaves, the highest thiols concentration was recorded in the polluted soil, with only GSH and cys-PC3 being observed (Table 1). However, in polluted soil with fertilizer, a diverse range of thiols was detected, although in lower amounts. Of note, GSH, the compound used by the plant to synthesize larger PCs, was observed overall. The concentration of GSH was decreased in both the roots and leaves of polluted soil with fertilizer, which is explained by the production of other kinds of thiols (Navazas et al., 2019), some of which were not possible to identify and therefore named CT1, CT2, and CT3 based on their retention time (Table 1). Despite the variation in the total thiols content between soil treatments, no significant differences were observed (Table 1). This is consistent with the accumulation of metal(loid)s in shoots, where no variations in As accumulation were detected (Fig. 4C).

Comparison of the total content of thiols revealed that the highest levels occurred in leaves (Table 1) while the greatest accumulation of metal(loid)s was in roots (Fig. 4D). This increase in NPT synthesis in leaves could be a plant defence mechanism to protect the photosynthetic system and avoid interference with the physiological and metabolic processes taking place in leaves (Lebrun et al., 2019). Similar results were reported by Fernández-Fuego et al. (2017a, 2017b) and Navazas et al. (2021), who worked with willow and birch grown in metal(loid)-polluted soils. Those authors proposed that, for the same amount of sample, leaves presented a larger number of metabolically active cells than roots, which have a higher proportion of lignified and suberized cells and, therefore, fewer physiologically active cells. However, plants have other detoxification mechanisms that may operate simultaneously with PCs, like organic acids (Fernández-Fuego et al., 2017a), phenols (Navazas et al., 2022). Another mechanism would be the binding of metal ions to cell walls, as occurs in *B. pubescens* when >90 % of accumulated metal(loid)s in roots are found in cell walls, which act as the major sinks for metal(loid)s (Fernández-Fuego et al., 2017a). Therefore, such mechanisms may explain why the translocation factor was below 1 in our study (Table S4).

3.6. Parameters related to oxidative stress

3.6.1. Photosynthetic pigments and photosynthetic efficiency

Photosynthetic pigments can be altered by the presence of metal (loid)s, in many cases resulting in chlorosis, which can lead to a reduction in photosynthetic capacity and even inhibition of photosynthesis. These effects might be due to the interruption of chlorophyll biosynthesis or inhibition of any enzyme of the metabolic pathway, leading to reduced CO_2 fixation and thus a decrease in plant growth (Abbas et al., 2018; Navazas et al., 2019; Kaya et al., 2022).

The chlorophyll *a* analysis revealed no differences in the content of chlorophyll *a*, b, or total across the treatments (Table 2), thereby indicating that the addition of the amendments did not affect pigment synthesis. However, an increase in carotenoids in S2F was observed when compared with S2 or S2R (Table 2). These findings may be explained by the antioxidant function of these molecules, which act on the harmful effects caused by the accumulation of As and Hg in leaves (Fig. 4C, D) (Patel et al., 2018; Baragaño et al., 2022). The ratio of carotenoids to total chlorophyll content was quite low and similar in all treatments (Table 2). These observations, according to Pistelli et al. (2017), would be indicative of a low-oxidative stress situation.

Photosynthetic efficiency (F_v/F_m) was slightly reduced in S2F and S2R, although this could not be attributed to the accumulation of As in shoots since no differences were observed between treatments, except for a higher Hg concentration in shoots of S2R treatments (Fig. 4C). The highest accumulation of As was observed in the roots of S2F (Fig. 4D), which could potentially impact the photosynthetic process by decreasing phosphate uptake, thereby limiting ATP synthesis during photosynthesis (Lin et al., 2020). The photosynthetic efficiency values of all treatments were within the limits considered normal (0.75–0.85) and therefore plant metabolism was not affected (Sánchez-Moreiras et al., 2020; Ye et al., 2023). Once again, the data demonstrated the remarkable resistance and tolerance of birch to the elevated concentrations of As and Hg present in S2.

3.6.2. Measurements of hydrogen peroxide, lipid peroxidation, and free proline

Metal(loid)s are potent pro-oxidants and plant exposure to them induces the production of reactive oxygen species (ROS), which in turn

Table 2
Photosynthetic pigment content (μg g^{-1} FW) and photosynthetic efficiency (F_v/F_m) in *B. pubescens* leaves after 60 days growing in soil S2 and its different treatments. Different letters in the same row indicate significant differences between treatments. S2, moderately contaminated soil; S2F, fertilizer-treated soil; S2R, byproduct-amended soil.

Treatments	S2	S2F	S2R
Total Chlorophyll (Chl)	1212.57 ± 5.42a	1195.18 ± 8.08a	1213.35 ± 5.74a
Chlorophyll a	639.94 ± 0.81a	644.50 ± 1.64a	640.38 ± 0.96a
Chlorophyll b	572.63 ± 6.15a	550.69 ± 9.7a	572.97 ± 6.68a
Carotenoids (Ct)	58.71 ± 2.50b	69.35 ± 4.35a	57.41 ± 2.92b
Ct/Total Chl	0.048 ± 0.002a	0.058 ± 0.004a	0.047 ± 0.002a
F_v/F_m	0.81 ± 0.001a	0.79 ± 0.008b	0.787 ± 0.005b

causes the peroxidation of membrane lipids and damage to proteins, amino acids, nucleic acids, and cell membranes (Berni et al., 2019). An increase in the ROS hydrogen peroxide (H_2O_2) is indicative of oxidative stress (Cuypers et al., 2016). Analysis of H_2O_2 in the birch samples revealed a reduction when soil was amended with fertilizer and byproducts when compared to S2 (Fig. 5A) and only an increase was observed in S2R shoots. In S2F, a decrease in H_2O_2 content was observed in all plant organs, particularly in roots and leaves. Notably, roots exhibited the highest accumulation of As (Fig. 4C, D). These findings suggest that the fertilizer played a role in alleviating oxidative stress induced by As and Hg, as it supplied essential nutrients to the plants. Alternatively, under these conditions, it is plausible that the antioxidant system of *B. pubescens* effectively countered the production of H_2O_2, which is evidenced by the elevated levels of carotenoids and proline observed (Table 2 and Fig. 5C). This is supported by the results of studies on other plant species (Sytar et al., 2013; Leão et al., 2014; Cuypers et al., 2016). On the other hand, it cannot be ruled out that an increase in antioxidant enzymes such as catalase and peroxidases (Abbas et al., 2018) could also contribute to reducing stress caused by As and Hg. However, these enzymes were not measured in the current study.

Malondialdehyde (MDA) is a marker of lipid peroxidation because it is released after the oxidation of fatty acids, which make up cell membranes in stressful situations such as the presence of contaminants in soil (Sytar et al., 2013; Anjum et al., 2015). Analysis of MDA content revealed a decrease in all the treatments and in all the plant organs tested when compared to plants grown in untreated soil (Fig. 5B). The fertilizer treatment (S2F) showed a lower concentration of MDA in stems and roots than the other treatments (Fig. 5B). These results could be explained by the nutrients provided by the fertilizer, which allowed plants to grow in more favourable conditions and reduce oxidative damage (Lebrun et al., 2019; Baragaño et al., 2022). Moreover, these results are contrary to those reported by Zhao et al. (2023), who suggested a direct correlation between metal(loid) accumulation in plant tissues and an increase in MDA content. On the other hand, S2R plants showed a decrease in H_2O_2 and MDA content, above all in roots. This finding indicates that the addition of byproducts leads to the immobilization of As (Ayala and Fernández, 2020), reducing its accumulation and also decreasing oxidative stress, as described in other studies using other metal(loid)-immobilizing amendments (Lebrun et al., 2019; Baragaño et al., 2022).

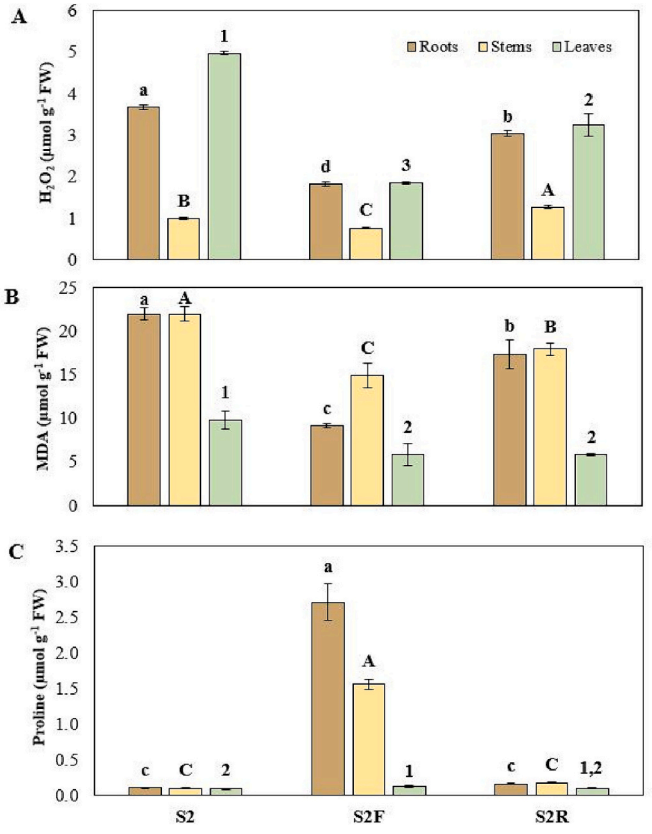

Fig. 5. Concentrations of H_2O_2 (A), MDA (B), and proline (C) in the leaves, stems and roots of *B. pubescens* after 60 days growing in soil S2 and its different treatments. Different lower-case letters indicate significant differences between treatments for roots, capital letters indicate significant differences between treatments for shoots, and numbers indicate significant differences between treatments for leaves. S2, moderately contaminated soil; S2F, fertilizer- treated soil; S2R, byproduct-amended soil.

One of the plant defence mechanisms against metal(loid) presence is the synthesis of a variety of enzymes and other metabolites, such as amino acids, peptides, and amines with chelating capacity and antioxidant properties (Martí et al., 2009). Some of these metabolites, such as free proline, could chelate metal(loid)s inside plant cells but mainly protect the integrity of cell membranes and scavenge ROS, thus reducing the oxidative damage caused by free hydroxyl radicals (Khedr et al., 2003; Sytar et al., 2013). Analysis of the proline content revealed no differences between the S2 and S2R treatments or across the different organs of the plant. However, the S2F treatment was the only one to show a large increase in proline in all plant organs, but mainly in roots and shoots (Fig. 4C). Such an increase in roots could be related to the previously mentioned higher accumulation of As, could also explain the decrease in H_2O_2 and MDA content, and finally could diminish the harmful effects of metal(loid)s (Fernández et al., 2013; Chen et al., 2015; Baragaño et al., 2022).

3.7. Deciphering the mechanism of Hg immobilization by coal fly ash

The immobilization of Hg in polluted soils through the application of soil amendments remains unclear as it is contingent upon the properties of the amendments, Hg concentration and speciation, as well as soil properties (Janeiro-Tato et al., 2021). Various techniques, such as sequential extraction, thermal desorption (TD), or XAS methods, have been described in the literature (McLaga et al., 2022). However, the application of a reactive permeable barrier (RPB) has allowed the analysis of Hg speciation in the Hg retained on it through HgTPD, comparing it with the Hg reference compounds (Fig. 6). This approach facilitates the identification of the mechanisms behind Hg immobilization in the amendments. Notably, changes in Hg speciation in the soil were not assessed, as total Hg content might hide alterations induced by the amendments, and the influence of roots could further complicate speciation determination.

Conversely, the coal fly ash from the RPB showed low concentrations of Hg, prompting its characterization. The coal fly ash had a surface area of 12 m^2/g and a LOI of 2.2 %, consistent with the characterization of coal fly ash from the same region (Abad-Valle et al., 2011). Furthermore, that study reported the presence of Hg in this material, a finding that is consistent with our sample, which contained a low Hg content (2 mg kg^{-1}) that can be considered negligible when compared with RPB, that showed a concentration of 22 mg kg^{-1} Hg. The assessment of the Hg speciation of byproducts (Fig. 6b) revealed the predominance of HgS and Hg-OM. This finding aligns with the Hg speciation reported for coal fly ash in the literature (López-Antón et al., 2011). In contrast, the determination of Hg speciation in the RPB indicated the presence of Hg-chloride species (Fig. 6b). These findings can be attributed to the mobility of the Hg species from soil (Janeiro-Tato et al., 2021) and its subsequent interaction with the chloride present in the coal fly ashes. Previous studies have demonstrated the effectiveness of capturing Hg in fly ash from flue gas (López-Antón et al., 2009). Nevertheless, it must be remembered that HgTPD provides information on thermally related binding strength but does not estimate the mobility of Hg in the liquid phase. Therefore, the formation of inorganic Hg species such as $HgCl_2$

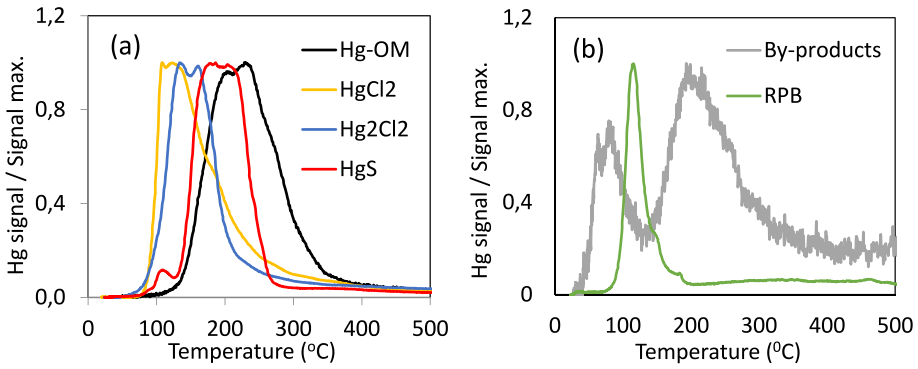

Fig. 6. Hg thermal decomposition profiles of a) Hg reference compounds (Hg-OM, HgS, $HgCl_2$, and Hg_2Cl_2) and b) pure by-products and Hg-enriched RPB.

and/or Hg stable compounds such as Hg_2Cl_2 cannot be ruled out.

4. Conclusions

The remediation of soils using steelmaking slag and coal fly ash increased soil pH and decreased the availability of As and Hg, achieving >50 % immobilization. Additionally, the use of these byproducts as components of a PRB beneath the soil layer minimized the presence of As and Hg in leachates. In the highly contaminated soil from "La Soterraña", plant damage and death were attributed to the high concentration of As and Hg in shoots and roots. Moreover, the presence of a PRB impeded proper water drainage, leading to irreversible alterations that ultimately killed the plants. Therefore, while reactive permeable barriers are useful for preventing pollutants from leaching into groundwater, caution should be exercised when combining them with phytoremediation.

Although the highest accumulation of As and Hg occurred in roots, the highest production of NPTs was detected in shoots, thereby pointing to a fundamental plant defence mechanism against high concentrations of metal(loid)s. The simultaneous use of organic fertilizer and byproducts as an amendment reduced oxidative stress by decreasing the H_2O_2 and MDA content in the plants. The increase in antioxidant compounds, such as carotenoids and free proline, after the applications of fertilizer revealed the plant's protective system against the high accumulation of metal(loid)s.

The assessment of the Hg speciation in the byproducts included in the reactive permeable barrier indicated that Hg was efficiently sequestered from the leachates by the coal fly ash, predominantly in the form of Hg—Cl species.

In conclusion, the steelmaking slag and coal fly ash used in this study show promise as amendments for As and Hg immobilization in highly contaminated soils within the framework of the circular economy. These amendments could be combined with phytoremediation techniques involving *B. pubescens* in soil moderately polluted by these contaminants.

CRediT authorship contribution statement

S. Sánchez: Writing – original draft, Formal analysis, Data curation. **D. Baragaño:** Writing – review & editing, Supervision, Formal analysis, Data curation, Conceptualization. **J.R. Gallego:** Writing – review & editing, Resources, Funding acquisition. **M.A. López-Antón:** Writing – review & editing, Resources, Funding acquisition. **R. Forján:** Writing – review & editing, Formal analysis, Data curation. **A. González:** Writing – review & editing, Supervision, Formal analysis, Data curation, Conceptualization.

Declaration of competing interest

The authors declare that they have no known competing financial interests or personal relationships that could have appeared to influence the work reported in this paper.

Data availability

Data will be made available on request.

Acknowledgments

This work was supported mainly by the project LIFE16ENV/ES/000481 (By-products4LIFE) and was partially financed by the Ministerio de Economía y Competitividad (MINECO, Spain) under the projects I+D+i PID2020-113558RB-C43 (MCIN/AEI/10.13039/501100011033) and NATURESOIL (AEI/Spain, NextGeneration EU, TED2021-130375B-I00). Diego Baragaño acknowledges the grant JDC2022-050209-I funded by MICIU/AEI/10.13039/501100011033 and by ESF+.

Appendix A. Supplementary data

Supplementary data to this article can be found online at https://doi.org/10.1016/j.scitotenv.2024.172297.

References

Abad-Valle, P, López-Antón, M.A., Díaz-Somoano, M., Martínez-Tarazona, M.R. (2011). The role of unburned carbon concentrates from fly ashes in the oxidation and retention of mercury. Chem. Eng. J., 174*(1),* 86–92. doi:https://doi.org/10.1016/j.cej.2011.08.053.

Abbas, G., Murtaza, B., Bibi, I., Shahid, M., Niazi, N.K., Khan, M.I., Amjad, M., Hussain, M., Natasha., 2018. Arsenic uptake, toxicity, detoxification, and speciation in plants: physiological, biochemical, and molecular aspects. Int. J. Environ. Res. Public Health 15 (1). https://doi.org/10.3390/ijerph15010059.

Anjum, N.A., Singh, H.P., Khan, M.I.R., Masood, A., 2015. Too much is bad — an appraisal of phytotoxicity of elevated plant-beneficial heavy metal ions. Environ. Sci. Pollut. Res. 22, 3361–3382. https://doi.org/10.1007/s11356-014-3849-9.

Aparicio, J. D., Raimondo, E. E., Sáez, J. M., Costa-Gutierrez, S. B., Alvarez, A., Benimeli, C. S., & Polti, M. A. (2022). The current approach to soil remediation : A review of physicochemical and biological technologies , and the potential of their strategic combination. *Journal of Environmental* Chem. Eng., 10(107141). doi:https://doi.org/10.1016/j.jece.2022.107141.

Arabi, Z., Rinklebe, J., El-Naggar, A., Hou, D., Sarmah, A.K., Moreno-Jiménez, E., 2021. (Im)mobilization of arsenic, chromium, and nickel in soils via biochar: A meta-analysis. Environ. Pollut. 286 (May) https://doi.org/10.1016/j.envpol.2021.117199.

Ayala, J., Fernández, B., 2020. Industrial waste materials as adsorbents for the removal of as and other toxic elements from an abandoned mine spoil heap leachate: a case study in Asturias. J. Hazard. Mater. 384 (121446), 121446 https://doi.org/10.1016/j.jhazmat.2019.121446.

Bali, A.S., Sidhu, G.P.S., 2021. Arsenic acquisition, toxicity and tolerance in plants - from physiology to remediation: A review. Chemosphere 283 (131050). https://doi.org/10.1016/j.chemosphere.2021.131050.

Baragaño, D., Forján, R., Álvarez, N., Gallego, J.R., González, A., 2022. Zero valent iron nanoparticles and organic fertilizer assisted phytoremediation in a mining soil: arsenic and mercury accumulation and effects on the antioxidative system of Medicago sativa L. J. Hazard. Mater. 433, 128748 https://doi.org/10.1016/j.jhazmat.2022.128748.

Bashir, S., Salam, A., Rehman, M., Khan, S., Gulshan, A.B., Iqbal, J., Shaaban, M., Mehmood, S., Zahra, A., Hu, H., 2019. Effective role of biochar, zeolite and steel slag

on leaching behavior of cd and its fractionations in soil column study. Bull. Environ. Contam. Toxicol. 102 (4), 567–572. https://doi.org/10.1007/s00128-019-02573-6.
Berni, R., Luyckx, M., Xu, X., Legay, S., Sergeant, K., 2019. Reactive oxygen species and heavy metal stress in plants: impact on the cell wall and secondary metabolism. Environ. Exp. Bot. 161, 98–106. https://doi.org/10.1016/j.envexpbot.2018.10.017.
Bhaduri, A.M., Fulekar, M.H., 2012. Antioxidant enzyme responses of plants to heavy metal stress. Rev. Environ. Sci. Biotechnol. 11, 55–69. https://doi.org/10.1007/s11157-011-9251-x.
Boente, C., Baragaño, D., García-González, N., Forján, R., Colina, A., Gallego, J.R., 2022. A holistic methodology to study geochemical and geomorphological control of the distribution of potentially toxic elements in soil. Catena 208. https://doi.org/10.1016/j.catena.2021.105730.
Bolan, N., Kunhikrishnan, A., Thangarajan, R., Kumpiene, J., Park, J., Makino, T., Beth, M., Scheckel, K., 2014. Remediation of heavy metal(loid)s contaminated soils – to mobilize or to immobilize? J. Hazard. Mater. 266, 141–166. https://doi.org/10.1016/j.jhazmat.2013.12.018.
BOPA, 2014. Resolución de 20 de marzo de 2014, de la Consejería de Fomento, Ordenación del Territorio y Medio Ambiente, por la que se establecen los Niveles Genéricos de Referencia para metales pesados en Suelos del Principado de Asturias. BOPA (Boletín Oficial Del Principado de Asturias) 91, 1–3.
Bortoloti, G.A., Baron, D., 2022. Phytoremediation of toxic heavy metals by Brassica plants: A biochemical and physiological approach. Environmental Advances 8 (February), 100204. https://doi.org/10.1016/j.envadv.2022.100204.
Breure, A.M., Lijzen, J.P.A., Maring, L., 2018. Soil and land management in a circular economy. Sci. Total Environ. 624 (2018), 1025–1030. https://doi.org/10.1016/j.scitotenv.2017.12.137.
Chandrakar, V., Naithani, S.C., Keshavkant, S., 2016. Arsenic-induced metabolic disturbances and their mitigation mechanisms in crop plants: A review. Biologia 71 (4), 367–377. https://doi.org/10.1515/biolog-2016-0052.
Chen, F., Wang, S., Mou, S., Azimuddin, I., Zhang, D., Pan, X., Al-Misned, F.A., Mortuza, M.G., 2015. Physiological responses and accumulation of heavy metals and arsenic of Medicago sativa L. growing on acidic copper mine tailings in arid lands. J. Geochem. Explor. 157, 27–35. https://doi.org/10.1016/j.gexplo.2015.05.011.
Cuypers, A., Hendrix, S., dos Reis, R.A., De Smet, S., Deckers, J., Gielen, H., Jozefczak, M., Loix, C., Vercampt, H., Vangronsveld, J., Keunen, E., 2016. Hydrogen peroxide, signaling in disguise during metal phytotoxicity. *Frontiers*. Plant Sci. 7 (APR2016) https://doi.org/10.3389/fpls.2016.00470.
Demiral, T., Turkan, I., 2005. Comparative lipid peroxidation, antioxidant defense systems and proline content in roots of two rice cultivars differing in salt tolerance. Environ. Exp. Bot. 53, 247–257. https://doi.org/10.1016/j.envexpbot.2004.03.017.
Demmig-Adams, B., Adams, W.W.I., 1996. Xanthophyll cycle and light stress in nature: uniform response to excess direct sunlight among higher plant species. Planta 198 (3), 460–470.
Dennis, K.K., Uppal, K., Liu, K.H., Ma, C., Liang, B., Go, Y.M., Jones, D.P., 2019. Phytochelatin database: A resource for phytochelatin complexes of nutritional and environmental metals. Database 2019 (1), 1–9. https://doi.org/10.1093/database/baz083.
Díaz, A.M., Forján, R., Gallego, J.R., Benavente-Hidalgo, L., Menéndez-Aguado, J.M., Baragaño, D., 2023. Nanoscale zero - valent iron mitigates arsenic mobilization and accumulation in Sinapis alba grown on a metal (loid)- polluted soil treated with a dunite mining waste - compost amendment. Plant and Soil 0123456789. https://doi.org/10.1007/s11104-023-05879-x.
Ellman, G.L., 1959. Tissue sulfhydryl groups. Arch. Biochem. Biophys. 82 (1), 70–77. https://doi.org/10.1016/0003-9861(59)90090-6.
Evers, D.C., Keane, S.E., Basu, N., Buck, D., 2016. Evaluating the effectiveness of the Minamata convention on mercury: principles and recommendations for next steps. Sci. Total Environ. 569–570, 888–903. https://doi.org/10.1016/j.scitotenv.2016.05.001.
FAO, & ITPS. (2015). *Status of the World's Soil Resources (SWSR)*. Technical Summary. Food and Agriculture Organization of the United Nations and Inter- governmental Technical Panel on Soils. http://www.fao.org/ documents/card/en/c/c6814873-efc3-41db-b7d3-2081a10ede50/.
Fernández, R., Bertrand, A., García, J.I., Tamés, R.S., González, A., 2012. Lead accumulation and synthesis of non-protein thiolic peptides in selected clones of Melilotus alba and Melilotus officinalis. Environ. Exp. Bot. 78, 18–24. https://doi.org/10.1016/j.envexpbot.2011.12.016.
Fernández, R., Bertrand, A., Reis, R., Mourato, M.P., Martins, L.L., González, A., 2013. Growth and physiological responses to cadmium stress of two populations of Dittrichia viscosa (L.) Greuter. J. Hazard. Mater. 244–245, 555–562. https://doi.org/10.1016/j.jhazmat.2012.10.044.
Fernández, B., Lara, L.M., Menéndez-Aguado, J.M., Ayala, J., García-González, N., Salgado, L., Colina, A., Gallego, J.L.R., 2020. A multi-faceted, environmental forensic characterization of a paradigmatic brownfield polluted by hazardous waste containing hg, as, PAHs and dioxins. Sci. Total Environ. 726 (138546), 1–12. https://doi.org/10.1016/j.scitotenv.2020.138546.
Fernández-Fuego, D., Bertrand, A., González, A., 2017a. Metal accumulation and detoxification mechanisms in mycorrhizal Betula pubescens. Environ. Pollut. 231, 1153–1162. https://doi.org/10.1016/j.envpol.2017.07.072.
Fernández-Fuego, D., Keunen, E., Cuypers, A., Bertrand, A., González, A., 2017b. Mycorrhization protects Betula pubescens Ehr. From metal-induced oxidative stress increasing its tolerance to grow in an industrial polluted soil. J. Hazard. Mater. 336, 119–127. https://doi.org/10.1016/j.jhazmat.2017.04.065.
Gallego, J.R., Esquinas, N., Rodríguez-valdés, E., Menéndez-aguado, J.M., Sierra, C., 2015. Comprehensive waste characterization and organic pollution co-occurrence in a hg and as mining and metallurgy brownfield. J. Hazard. Mater. 300, 561–571. https://doi.org/10.1016/j.jhazmat.2015.07.029.
Gąsecka, M., Drzewiecka, K., Magdziak, Z., Piechalak, A., Budka, A., Waliszewska, B., Szentner, K., Goliński, P., Niedzielski, P., Budzyńska, S., Mleczek, M., 2021. Arsenic uptake, speciation and physiological response of tree species (Acer pseudoplatanus, Betula pendula and Quercus robur) treated with dimethylarsinic acid. Chemosphere 263 (127859), 1–20. https://doi.org/10.1016/j.chemosphere.2020.127859.
Gil-Díaz, M., Rodríguez-Valdés, E., Alonso, J., Baragaño, D., Gallego, J.R., Lobo, M.C., 2019. Nanoremediation and long-term monitoring of brownfield soil highly polluted with as and hg. Sci. Total Environ. 675, 165–175. https://doi.org/10.1016/j.scitotenv.2019.04.183.
González, H., Fernández-Fuego, D., Bertrand, A., González, A., 2019. Effect of pH and citric acid on the growth, arsenic accumulation, and phytochelatin synthesis in Eupatorium cannabinum L., a promising plant for phytostabilization. Environ. Sci. Pollut. Res. 26 (25), 26242–26253. https://doi.org/10.1007/s11356-019-05657-2.
González-Fernández, B., Rodríguez-Valdés, E., Boente, C., Menéndez-Casares, E., Fernández-Braña, A., Gallego, J.R., 2018. Long-term ongoing impact of arsenic contamination on the environmental compartments of a former mining-metallurgy area. Sci. Total Environ. 610–611, 820–830. https://doi.org/10.1016/j.scitotenv.2017.08.135.
Hazelton, P., Murphy, B., 2007. Interpreting soil test results what do all the numbers mean? In CSIRO Publishing. https://doi.org/10.1071/9781486303977.
Hudson-Edwards, K., 2016. Tackling mine wastes. Science 352 (6283), 288–290. https://doi.org/10.1126/science.aaf3354.
Jacob, M.J., Karthik, C., Ganesh, R., Kumar, S.S., Prabakar, D., Kadirvelu, K., Pugazhendhi, A., 2018. Biological approaches to tackle heavy metal pollution: A survey of literature. J. Environ. Manage. 217, 56–70. https://doi.org/10.1016/j.jenvman.2018.03.077.
Janeiro-Tato, I., Lopez-Anton, M.A., Baragaño, D., Antuña-Nieto, C., Rodríguez, E., Peláez, A.I., Gallego, J.R., Martínez-Tarazona, M.R., 2021. Immobilization of mercury in contaminated soils through the use of new carbon foam amendments. *Environmental sciences*. Europe 33 (1). https://doi.org/10.1186/s12302-021-00569-w.
Jozefczak, M., Remans, T., Vangronsveld, J., Cuypers, A., 2012. Glutathione is a key player in metal-induced oxidative stress defenses. Int. J. Mol. Sci. 13, 3145–3175. https://doi.org/10.3390/ijms13033145.
Kaya, C., Sarıoglu, A., Ashraf, M., Alyemeni, M.N., Ahmad, P., 2022. The combined supplementation of melatonin and salicylic acid effectively detoxifies arsenic toxicity by modulating phytochelatins and nitrogen metabolism in pepper plants. Environ. Pollut. 297 (November 2021), 118727 https://doi.org/10.1016/j.envpol.2021.118727.
Khedr, A.H.A., Abbas, M.A., Abdel Wahid, A.A., Quick, W.P., Abogadallah, G.M., 2003. Proline induces the expression of salt-stress-responsive proteins and may improve the adaptation of Pancratium maritimum L. to salt-stress. J. Exp. Bot. 54 (392), 2553–2562. https://doi.org/10.1093/jxb/erg277.
Koptsik, G.N., Koptsik, S.V., Smirnova, I.E., Sinichkina, M.A., 2021. Effect of Soil Degradation and Remediation in Technogenic Barrens on the Uptake of Nutrients and Heavy Metals by Plants in the Kola Subarctic. 54 (8), 1252–1264. https://doi.org/10.1134/S106422932108010X.
Leão, G.A., de Oliveira, J.A., Felipe, R.T.A., Farnese, F.S., Gusman, G.S., 2014. Anthocyanins, thiols, and antioxidant scavenging enzymes are involved in Lemna gibba tolerance to arsenic. J. Plant Interact. 9 (1), 143–151. https://doi.org/10.1080/17429145.2013.784815.
Lebrun, M., Miard, F., Nandillon, R., Scippa, G.S., Bourgerie, S., Morabito, D., 2019. Biochar effect associated with compost and iron to promote Pb and as soil stabilization and Salix viminalis L. growth. Chemosphere 222, 810–822. https://doi.org/10.1016/j.chemosphere.2019.01.188.
Lebrun, M., Nandillon, R., Miard, F., Scippa, G.S., Bourgerie, S., Morabito, D., 2021. Application of amendments for the phytoremediation of a former mine technosol by endemic pioneer species: alder and birch seedlings. Environ. Geochem. Health 43 (1), 77–89. https://doi.org/10.1007/s10653-020-00678-0.
León-Burgos, A.F., Unigarro, C.A., Balaguera-López, H.E., 2022. Soil waterlogging conditions affect growth, water status, and chlorophyll "a" fluorescence in coffee plants (Coffea arabica L.). Agronomy 12 (1270). https://doi.org/10.3390/agronomy12061270.
Lichtenthaler, H.K., Wellburn, A.R., 1983. Determinations of total carotenoids and chlorophylls a and b of leaf extracts in different solvents. Biochem. Soc. Trans. 11 (5), 591–592. https://doi.org/10.1042/bst0110591.
Lin, W., Lin, M., Zhou, H., Wu, H., Li, Z., Lin, W.L., 2019. The effects of chemical and organic fertilizer usage on rhizosphere soil in tea orchards. PloS One 14 (5), 1–16.
Lin, J., Gao, X., Zhao, J., Zhang, J., Chen, S., Lu, L., 2020. Plant cadmium resistance 2 (SaPCR2) facilitates cadmium efflux in the roots of Hyperaccumulator Sedum alfredii Hance. Front. Plant Sci. 11 (October), 1–11. https://doi.org/10.3389/fpls.2020.568887.
Liu, G., Meng, J., Huang, Y., Dai, Z., Tang, C., Xu, J., 2020. Effects of carbide slag, lodestone and biochar on the immobilization, plant uptake and translocation of as and cd in a contaminated paddy soil. Environ. Pollut. 266, 115194 https://doi.org/10.1016/j.envpol.2020.115194.
López-Antón, M.A., Abad-Valle, P., Díaz-Somoano, M., Suárez-Ruiz, I., Martínez-Tarazona, M.R., 2009. The influence of carbon particle type in fly ashes on mercury adsorption. Fuel 88 (7), 1194–1200. https://doi.org/10.1016/j.fuel.2007.07.029.
López-Antón, M.A., Perry, R., Abad-Valle, P., Díaz-Somoano, M., Martínez-Tarazona, M. R., Maroto-Valer, M.M., 2011. Speciation of mercury in fly ashes by temperature programmed decomposition. Fuel Process. Technol. 92 (3), 707–711. https://doi.org/10.1016/j.fuproc.2010.12.002.
Martí, M.C., Camejo, D., Fernández-García, N., Rellán-Álvarez, R., Marques, S., Sevilla, F., Jiménez, A., 2009. Effect of oil refinery sludges on the growth and

antioxidant system of alfalfa plants. J. Hazard. Mater. 171 (1–3), 879–885. https://doi.org/10.1016/j.jhazmat.2009.06.083.
Matanzas, N., Sierra, M.J., Afif, E., Díaz, T.E., Gallego, J.R., Millán, R., 2017. Geochemical study of a mining-metallurgy site polluted with as and hg and the transfer of these contaminants to Equisetum sp. J. Geochem. Explor. 182 (August), 1–9. https://doi.org/10.1016/j.gexplo.2017.08.008.
McLaga, D.S., Schwab, L., Wiederhold, J.G., Chen, L., Pietrucha, J., Kraemer, S.M., Biester, H., 2022. Demystifying mercury geochemistry in contaminated soil-groundwater systems with complementary mercury stable isotope, concentration, and speciation analyses. Environ Sci Process Impacts 24, 1406.
Medina, A., Gamero, P., Almanza, J.M., Vargas, A., Montoya, A., Vargas, G., Izquierdo, M., 2010. Fly ash from a Mexican mineral coal. II. Source of W zeolite and its effectiveness in arsenic (V) adsorption. J. Hazard. Mater. 181 (1–3), 91–104. https://doi.org/10.1016/j.jhazmat.2010.04.102.
Mishra, S., Alfeld, M., Sobotka, R., Andresen, E., Falkenberg, G., Küpper, H., 2016. Analysis of sublethal arsenic toxicity to Ceratophyllum demersum: subcellular distribution of arsenic and inhibition of chlorophyll biosynthesis. J. Exp. Bot. 67 (15), 4639–4646. https://doi.org/10.1093/jxb/erw238.
Mohan, T.C., Castrillo, G., Navarro, C., Zarco-fernández, S., Ramireddy, E., Mateo, C., Zamarreño, A.M., Paz-ares, J., Muñoz, R., García-mina, J.M., Hernández, L.E., Schmülling, T., Leyva, A., 2016. Cytokinin determines thiol-mediated arsenic tolerance and accumulation. Plant Physiol. 171, 1418–1426. https://doi.org/10.1104/pp.16.00372.
Mourato, M., Reis, R., Martins, L.L., 2012. Characterization of Plant Antioxidative System in Response to Abiotic Stresses: A Focus on Heavy Metal Toxicity (In Advances in selected plant physiology aspects).
Mourato, M., Pinto, F., Moreira, I., Sales, J., Leitão, I., Martins, L.L., 2019. The effect of cd stress in mineral nutrient uptake in plants. In: Cadmium Toxicity and Tolerance in Plants. Academic Press, pp. 327–348. https://doi.org/10.1016/B978-0-12-814864-8.00013-9.
Murashige, T., Skoog, F., 1962. A revised medium for rapid growth and bio assays with tobacco tissue cultures. Physiol. Plant. 15 (3), 473–497. https://doi.org/10.1111/j.1399-3054.1962.tb08052.x.
Natasha, Shahid, M., Khalid, S., Bibi, I., Bundschuh, J., Khan Niazi, N., Dumat, C., 2020. A critical review of mercury speciation, bioavailability, toxicity and detoxification in soil-plant environment: ecotoxicology and health risk assessment. Sci. Total Environ. 711, 134749 https://doi.org/10.1016/j.scitotenv.2019.134749.
Navazas, A., Hendrix, S., Cuypers, A., González, A., 2019. Integrative response of arsenic uptake, speciation and detoxification by Salix atrocinerea. Sci. Total Environ. 689, 422–433. https://doi.org/10.1016/j.scitotenv.2019.06.279.
Navazas, A., Thijs, S., Feito, I., Vangronsveld, J., Peláez, A.I., Cuypers, A., González, A., 2021. Arsenate-reducing bacteria affect as accumulation and tolerance in Salix atrocinerea. Sci. Total Environ. 769 (144648), 1–13. https://doi.org/10.1016/j.scitotenv.2020.144648.
Navazas, A., Mesa, V., Thijs, S., Fuente-Maqueda, F., Vangronsveld, J., Peláez, A.I., Cuypers, A., González, A., 2022. Bacterial inoculant-assisted phytoremediation affects trace element uptake and metabolite content in Salix atrocinerea. Sci. Total Environ. 820 (153088), 1–13. https://doi.org/10.1016/j.scitotenv.2022.153088.
Nirola, R., Megharaj, M., Palanisami, T., Aryal, R., Venkateswarlu, K., Naidu, Ravi, 2015. Evaluation of metal uptake factors of native trees colonizing an abandoned copper mine – a quest for phytostabilization. Journal of Sustainable Mining 14 (3), 115–123. https://doi.org/10.1016/j.jsm.2015.11.001.
Pal, R., Rai, J.P.N., 2010. Phytochelatins: peptides involved in heavy metal detoxification. Applied Biochemistry Biotechnology 160, 945–963. https://doi.org/10.1007/s12010-009-8565-4.
Pasricha, S., Mathur, V., Garg, A., Lenka, S., & Verma, K. (2021). Molecular mechanisms underlying heavy metal uptake , translocation and tolerance in hyperaccumulators-an analysis Heavy metal tolerance in hyperaccumulators. Environmental Challenges, 4(April), 100197. doi:https://doi.org/10.1016/j.envc.2021.100197.
Patel, A., Tiwari, S., Prasad, S.M., 2018. Toxicity assessment of arsenate and arsenite on growth, chlorophyll a fluorescence and antioxidant machinery in Nostoc muscorum. Ecotoxicol. Environ. Saf. 157 (April), 369–379. https://doi.org/10.1016/j.ecoenv.2018.03.056.
Payá-Peréz, A., Rodríguez-Eugenio, N., 2018. Status of local soil contamination in Europe: revision of the Indicator “Progress in the management contaminated sites in Europe”, EUR 29124 EN. Publications Office of the European Union. https://doi.org/10.2760/093804.
Pistelli, L., D'Angiolillo, F., Morelli, E., Basso, B., Rosellini, I., Posarelli, M., Barbafieri, M., 2017. Response of spontaneous plants from an ex-mining site of Elba island (Tuscany, Italy) to metal(loid) contamination. Environ. Sci. Pollut. Res. 24 (8), 7809–7820. https://doi.org/10.1007/s11356-017-8488-5.
Rucinska-Sobkowiak, R., 2016. Water relations in plants subjected to heavy metal stresses. Acta Physiologiae Plantarum 38 (257). https://doi.org/10.1007/s11738-016-2277-5.
Rumayor, M., López-Antón, M.A., Díaz-Somoano, M., Martínez-Tarazona, M.R., 2015. A new approach to mercury speciation in solids using a thermal desorption technique. Fuel 160 (15), 525–530. https://doi.org/10.1016/j.fuel.2015.08.028.
Sánchez-Moreiras, A.M., Graña, E., Reigosa, M.J., Araniti, F., 2020. Imaging of chlorophyll a fluorescence in natural compound-induced stress detection. Front. Plant Sci. 11 (December), 1–15. https://doi.org/10.3389/fpls.2020.583590.
Sarwar, N., Imran, M., Shaheen, M.R., Ishaque, W., Kamran, M.A., Matloob, A., Rehim, A., Hussain, S., 2017. Phytoremediation strategies for soils contaminated with heavy metals: modifications and future perspectives. Chemosphere 171, 710–721. https://doi.org/10.1016/j.chemosphere.2016.12.116.
Sharma, R., Bhardwaj, R., Handa, N., Gautam, V., Kohli, S.K., Bali, S., Kaur, P., Thukral, A.K., Arora, S., Ohri, P., Vig, A.P., 2016. Chapter 10 - responses of Phytochelatins and Metallothioneins in alleviation of heavy metal stress in plants: An overview. In: Ahmad, P.B.T.-P.M.I. (Ed.), Plant Metal Interaction. Elsevier, pp. 263–283. https://doi.org/10.1016/B978-0-12-803158-2.00010-2.
Singh, N., Ma, L.Q., Srivastava, M., Rathinasabapathi, B., 2006. Metabolic adaptations to arsenic-induced oxidative stress in Pteris vittata L and Pteris ensiformis L. Plant Sci. 170 (2), 274–282. https://doi.org/10.1016/j.plantsci.2005.08.013.
Souri, Z., Karimi, N., Sandalio, L.M., 2017. Arsenic Hyperaccumulation strategies: an overview. Frontiers in Cell and Developmental Biology 5 (67), 1–8. https://doi.org/10.3389/fcell.2017.00067.
Souza Neto, H. F. de, Pereira, W. V. da S., Dias, Y. N., Souza, E. S. de, Teixeira, R. A., Lima, M. W. de, Ramos, S. J., Amarante, C. B. do, & Fernandes, A. R. (2020). Environmental and human health risks of arsenic in gold mining areas in the eastern Amazon. Environ. Pollut., 265, 114969. doi:https://doi.org/10.1016/j.envpol.2020.114969.
Sytar, O., Kumar, A., Latowski, D., 2013. Heavy metal-induced oxidative damage, defense reactions, and detoxification mechanisms in plants. Acta Physiol. Plant. 35, 985–999. https://doi.org/10.1007/s11738-012-1169-6.
Taran, N., Shevtsova, T., Sytar, O., 2020. Heavy metal pollution: Effect on plants and food. In: Landi, M., Shemet, S.A., Fedenko, V.S. (Eds.), Metal Toxicity in Higher Plantas. Nova Science Publishers, pp. 1–20.
Triassi, M., Cerino, P., Montuori, P., Pizzolante, A., Trama, U., Nicodemo, F., D'Auria, J. L., De Vita, S., De Rosa, E., Limone, A., 2023. Heavy metals in groundwater of southern Italy: occurrence and potential adverse effects on the environment and human health. Int. J. Environ. Res. Public Health 20 (1693). https://doi.org/10.3390/ijerph20031693.
USEPA (U.S. Environmental Protection Agency). (1992). *Method 1311: Toxicity Characteristic Leaching Procedure* (Vol. 1311).
Viehweger, K., 2014. How plants cope with heavy metals. Bot. Stud. 55.
Wang, Y., Tsang, D.C.W., 2013. Effects of solution chemistry on arsenic (V) removal by low-cost adsorbents. J. Environ. Sci. (China) 25 (11), 2291–2298. https://doi.org/10.1016/S1001-0742(12)60296-4.
Wang, Q., Huang, Q., Guo, G., Qin, J., 2020. Reducing bioavailability of heavy metals in contaminated soil and uptake by maize using organic-inorganic mixed fertilizer. Chemosphere 261 (128122). https://doi.org/10.1016/j.chemosphere.2020.128122.
Wang, Z., Luo, P., Zha, X., Xu, C., Kang, S., Zhou, M., Nover, D., Wang, Y., 2022. Overview assessment of risk evaluation and treatment technologies for heavy metal pollution of water and soil. J. Clean. Prod. 379 (134043) https://doi.org/10.1016/j.jclepro.2022.134043.
White, P.J., Brown, P.H., 2010. Plant nutrition for sustainable development and global health. Ann. Bot. 105 (7), 1073–1080. https://doi.org/10.1093/aob/mcq085.
Ye, D., Wu, L., Xiaobin, L., Opeyemi Atoba, T., Wu, W., Weng, H., 2023. A synthetic review of various dimensions of non-destructive plant stress phenotyping. Plants 12 (1698).
Zagorchev, L., Seal, C.E., Kranner, I., Odjakova, M., 2013. A central role for thiols in plant tolerance to abiotic stress. Int. J. Mol. Sci. 14, 7405–7432. https://doi.org/10.3390/ijms14047405.
Zhang, J., Hamza, A., Xie, Z., Hussain, S., Brestic, M., Ali, M., Ulhassan, Z., Yu, M., Allakhverdiev, S.I., Shabala, S., 2021. Arsenic transport and interaction with plant metabolism: clues for improving agricultural productivity and food safety. Environ. Pollut. 290 (117987) https://doi.org/10.1016/j.envpol.2021.117987.
Zhao, R., Cao, X., Li, X., Li, T., Zhang, H., Cui, X., Cui, Z., 2023. Ecological toxicity of cd, Pb, Zn, hg and regulation mechanism in Solanum nigrum L. Chemosphere 313 (December 2022), 137447. https://doi.org/10.1016/j.chemosphere.2022.137447.